

Three-Dimensional Quantification of Myocardial Collagen Morphology from Confocal Images

Abdallah I. Hasaballa¹(✉), Gregory B. Sands^{1,2}, Alexander J. Wilson^{1,2}, Alistair A. Young^{1,3}, Vicky Y. Wang¹, Ian J. LeGrice^{1,2}, and Martyn P. Nash^{1,4}

¹ Auckland Bioengineering Institute, University of Auckland, Auckland, New Zealand
ahas804@aucklanduni.ac.nz

² Department of Physiology, University of Auckland, Auckland, New Zealand

³ Department of Anatomy with Radiology, University of Auckland,
Auckland, New Zealand

⁴ Department of Engineering Science, University of Auckland,
Auckland, New Zealand

Abstract. The mechanical properties of myocardial tissue are primarily determined by the organisation of the collagen network. Quantitative measurements of collagen morphology can help to understand the structure-function relationship in cardiac tissue. In this study, we segmented collagen from high-resolution three-dimensional (3D) images of the left ventricle (LV) mid-wall myocardium obtained using extended-volume confocal microscopy. 3D shape analysis was used to compute the morphological parameters elongation (e), flatness (f), and anisotropy (a). We applied this analysis to both control and hypertensive rat hearts and showed distinct differences between the control and remodelled hearts, particularly in collagen elongation. The predominant form of collagen in the control rat is elongated with a value of $e = 0.846 \pm 0.041$, whereas in the hypertensive rat collagen, is arranged mostly in a sheet-like form with $e = 0.301 \pm 0.023$. Such quantitative information can be used to develop microstructural models of the myocardium that link the observed changes in cardiac microstructure to changes in mechanical function during the progression of heart diseases, which will help to elucidate the underlying pathological mechanisms.

Keywords: Collagen morphology · Seeded region-growing algorithm · Shape analysis · Moments of inertia · Confocal imaging

1 Introduction

The mechanical behaviour of the myocardium is mainly dependent on the organisation of myocytes and the composition of the cardiac extracellular matrix (ECM). Collagen is the predominant structural component of ECM and the major stress-bearing component of passive myocardium [1]. Consequently, any change in the collagen architecture is often associated with a pathological function such as is observed in hypertensive hearts [2]. Therefore, it is important to

have quantitative information on collagen morphology in order to develop a better understanding of the relationship between the microstructure and mechanical function of the myocardium.

The role of the collagen structure in myocardial function has been investigated by many research groups [3, 4] using animal models, such as the spontaneously hypertensive rat (SHR) [5, 6]. The SHR is a well-established model of genetic hypertension that develops with aging, and leads to myocardial changes that reflect those seen in hypertensive human hearts. In studies using high-resolution extended volume confocal microscopy, it has been shown that aged SHRs have significant changes in myocardial architecture when compared to age-matched control Wistar-Kyoto (WKY) rats [6]. These structural changes include myocyte hypertrophy, an increase in the amount of collagen, and a loss of myocardial laminar organisation because of the scarring together of collagen strands, which line the cleavage planes between laminae. These alterations in the myocardial structure are believed to lead to impaired myocardial mechanical function and, hence, reduced cardiac performance.

In this study, we have developed a novel method to quantify collagen morphology in the tissue blocks of the mid-wall of the left ventricle (LV) myocardium taken from a 12-month-old WKY rat and an age-matched SHR. Preliminary results on differences in structural and morphological parameters between WKY and SHR are presented and discussed.

2 Methods

In order to quantify collagen morphology, collagen was segmented from images of the rat LV free wall, and morphological parameters describing elongation, flatness, and anisotropy were computed at 50,000 randomly selected collagen locations within each image volume.

2.1 3D Tissue Images

Blocks of LV wall from a 12-month-old WKY rat and an age-matched SHR were labelled with picosirius red to highlight collagen, embedded in resin, mounted on a high-precision three-axis stage and imaged using laser scanning confocal microscopy. The imaging protocol and technique have been described in detail elsewhere [7]. Although this imaging technique is time-consuming and generates large datasets, it provides precise information at high spatial resolution about the 3D organisation of the myocytes and collagen network [8]. Representative 3D image volumes of the WKY rat and SHR used in this study are shown in Fig. 1. The 3D tissue blocks were imaged at a resolution of $1\ \mu\text{m}$ per voxel side and with a total volume of $(293\ \mu\text{m} \times 256\ \mu\text{m} \times 237\ \mu\text{m})$.

2.2 Collagen Segmentation

In order to segment the collagen network in the 3D volume images, we developed an image processing framework, which includes four main steps:

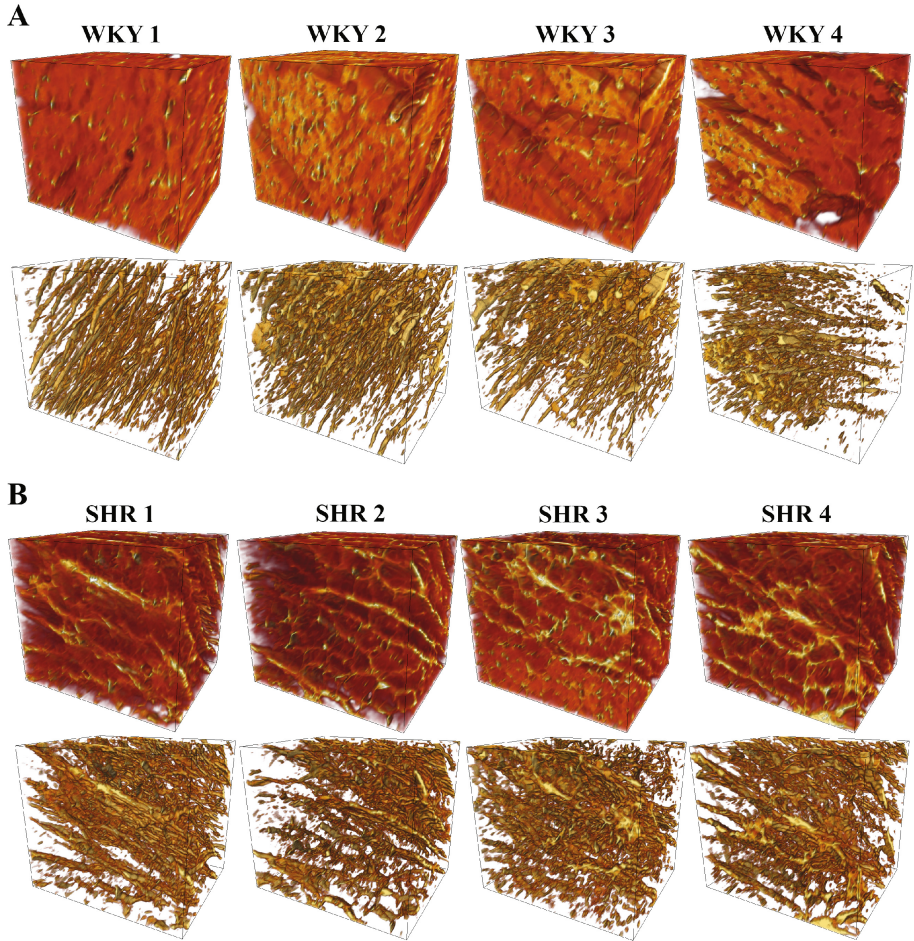


Fig. 1. 3D image volumes from (A) a 12-month-old WKY rat heart and (B) an age-matched SHR heart (*top*), together with the corresponding collagen structures (*bottom*). Collagen appears brighter, while myocytes have variable intensity.

- (i) **Adjustment of image intensity** (using the MATLAB¹ *imadjust* function). The *imadjust* function improves the intensity distribution of the image by mapping the input image's intensity values to a new range such that 1% of the data is saturated at low and high intensities of the input image.
- (ii) **Unsharp masking** (using the MATLAB *imsharpen* function). This function sharpens edges on the elements without increasing noise. The parameters used in this study were *radius* = 5, *amount* = 0.5 and *threshold* = 0.
- (iii) **Edge-preserving smoothing** (customised code in MATLAB as described by Weickert et al. in [9]). This step is very similar to a Gaussian filter as it

¹ The MathWorks, Inc., Natick, Massachusetts, United States.

smooths out the noise. Unlike the Gaussian filter, the diffusion in the neighbouring edges is reduced. Thus, it smooths the image while preserving edge information. The behaviour of this filter is controlled by two parameters: *contrast*, which determines how much the smoothing is reduced in the vicinity of the edges, and *kernel size*. The parameters used in this study were *contrast* = 3.5 and *kernel size* = 3.

(iv) **Entropy thresholding** (customised code in MATLAB following the entropy principles as explained in details in [10]). Entropy thresholding extracts a binary segmentation of the collagen.

The combination of these steps helps to preserve as much of the collagen information that is contained in the original image as possible. An example of automated collagen segmentation using the proposed framework is given in Fig. 2.

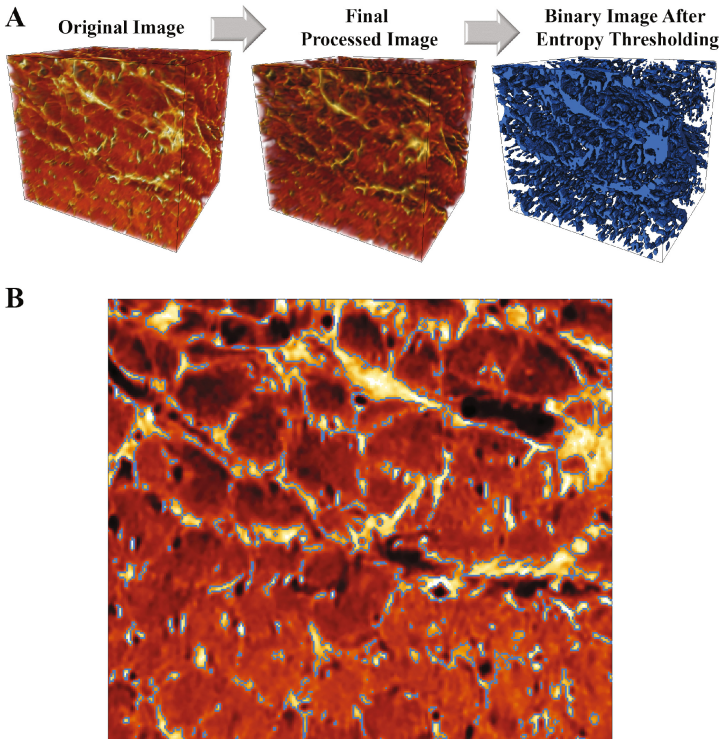


Fig. 2. Collagen segmentation in the 3D confocal images. (A) image segmentation steps. (B) cross section view of collagen segmentation boundaries overlaid on the original image. (Color figure online)

2.3 Region Extraction

Collagen morphology is described at a local level, therefore, we extracted a number of small sub-regions from the image block for quantification.

Distinct, random collagen locations were selected from the 3D segmented image block, and a cube (region of interest) was extracted with collagen voxel/point at the center of the cube (cubes were allowed to overlap). The collagen locations were randomly selected using the *randi* function in MATLAB, which creates uniformly distributed random locations within the 3D image bounds, and retained for analysis if the selected location had been classified as collagen. Finally, a 3D region-growing algorithm [11] was applied in each cube, which starts with the central collagen seed point identified above and grows with neighboring voxels of connected collagen.

The size of the region of interest was selected to be large enough to represent the microstructural organisation of the collagen accurately, yet small enough to only contain local information. In this study, the length of the cube was 25 μm . The number of cubes to be analysed was determined by progressively increasing the number of cubes until the results converged (i.e. no statistically significant differences with the addition of more cubes). Here, convergence was reached at 50,000 cubes.

2.4 Shape Analysis

Many imaging studies have used moments of inertia for shape analysis [12] and pattern recognition [13]. In a binary image, the first-order moments define the center of mass

$$M_{1x} = \sum_C x_i, \quad M_{1y} = \sum_C y_i, \quad M_{1z} = \sum_C z_i \quad (1)$$

where (x_i, y_i, z_i) is a point in the object C . Here, C is the segmented collagen object in the region of interest. The second-order moments are defined as

$$\begin{aligned} M_{2xx} &= \sum_C (x_i - M_{1x})^2, \\ M_{2yy} &= \sum_C (y_i - M_{1y})^2, \\ M_{2zz} &= \sum_C (z_i - M_{1z})^2, \\ M_{2xy} &= \sum_C (x_i - M_{1x})(y_i - M_{1y}), \\ M_{2yz} &= \sum_C (y_i - M_{1y})(z_i - M_{1z}), \\ M_{2xz} &= \sum_C (x_i - M_{1x})(z_i - M_{1z}) \end{aligned} \quad (2)$$

and the inertia matrix (covariance matrix) can be written as

$$M = \begin{bmatrix} M_{2xx} & M_{2xy} & M_{2xz} \\ M_{2xy} & M_{2yy} & M_{2yz} \\ M_{2xz} & M_{2yz} & M_{2zz} \end{bmatrix} \quad (3)$$

The eigenvalues of M provide a good indicator of shape. For example, when the three eigenvalues are similar, the shape tends to be spherical. The 3D morphological parameters in the range of $[0,1]$ were derived from the eigenvalues: elongation (e), flatness (f), and anisotropy (a)

$$e = 1 - \frac{\lambda_2}{\lambda_1}, \quad f = 1 - \frac{\lambda_3}{\lambda_2}, \quad a = 1 - \frac{\lambda_3}{\lambda_1} \quad (4)$$

where λ_1 denotes the primary eigenvalue of M , λ_2 denotes the secondary eigenvalue, and λ_3 denotes the tertiary eigenvalue such that $\lambda_1 \geq \lambda_2 \geq \lambda_3 > 0$.

The proposed framework for quantifying the 3D collagen morphology from confocal images of healthy and diseased hearts is summarised in Fig. 3.

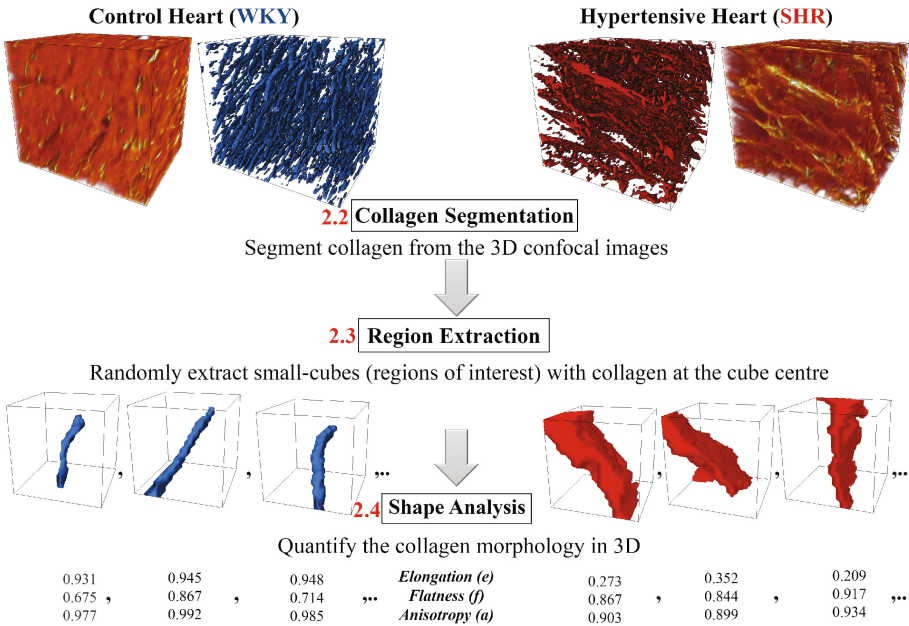


Fig. 3. A framework for quantification of collagen morphology in 3D.

3 Results and Discussion

The proposed framework for quantifying collagen morphology in 3D has been applied to four sets of confocal images from each of a control (WKY) rat heart

and a hypertensive rat (SHR) heart (see Fig. 1). The distributions of the three morphological parameters for all eight tissue blocks are shown in Fig. 4 and are similar within each animal group. There are distinct differences in the distributions of elongation between the WKY and SHR groups, whereas distributions of flatness and anisotropy in both groups are similar.

Figure 5(A) shows the 3D distribution density of the morphological parameters for WKY and SHR using heatmaps. The core locations and the patterns of density distribution are substantially different between WKY and SHR. The core centres which indicate the most common collagen form in WKY and SHR are given in Table 1. To illustrate the structural differences between WKY and SHR, four small cubes from the core of each heatmap for each case are shown in Fig. 5 (B). This comparative analysis revealed that the dominant collagen shape in WKY was elongated, whereas in SHR it had a sheet-like form. Such differences in the structure may explain the higher stiffness observed in SHR functional studies [5, 6]. From a mechanics perspective, the microstructural shape of composite materials has a considerable effect on the physical properties [14]. It seems likely that the increased stiffness observed in SHR hearts compared with those from normal animals is a consequence of collagen remodelling into sheet-like shapes in the SHR.

Table 1. Comparison of the mean and standard deviations (SDs) of the core centres for WKY and SHR.

| | Elongation | | Flatness | | Anisotropy | |
|-----|------------|-------|----------|-------|------------|-------|
| | Mean | SD | Mean | SD | Mean | SD |
| WKY | 0.846 | 0.041 | 0.771 | 0.053 | 0.967 | 0.002 |
| SHR | 0.301 | 0.023 | 0.833 | 0.016 | 0.883 | 0.001 |

There is a dearth of quantitative information available in the literature regarding the 3D morphology of collagen in the heart. Nevertheless, microstructural studies [6, 15] by LeGrice and colleagues have reported that the perimysial collagen organisation in WKY rat hearts is a network of collagen fibres and bundles, while the SHR, collagen forms dense sheets due to the fusion and thickening of perimysial collagen between adjacent myocardial layers. Our quantitative results are consistent with these observations.

A limitation of this study is that the automatic image analysis techniques are not able to distinguish between perimysial and endomysial collagen, and thus, the contributions of each type of collagen to the results could not be determined.

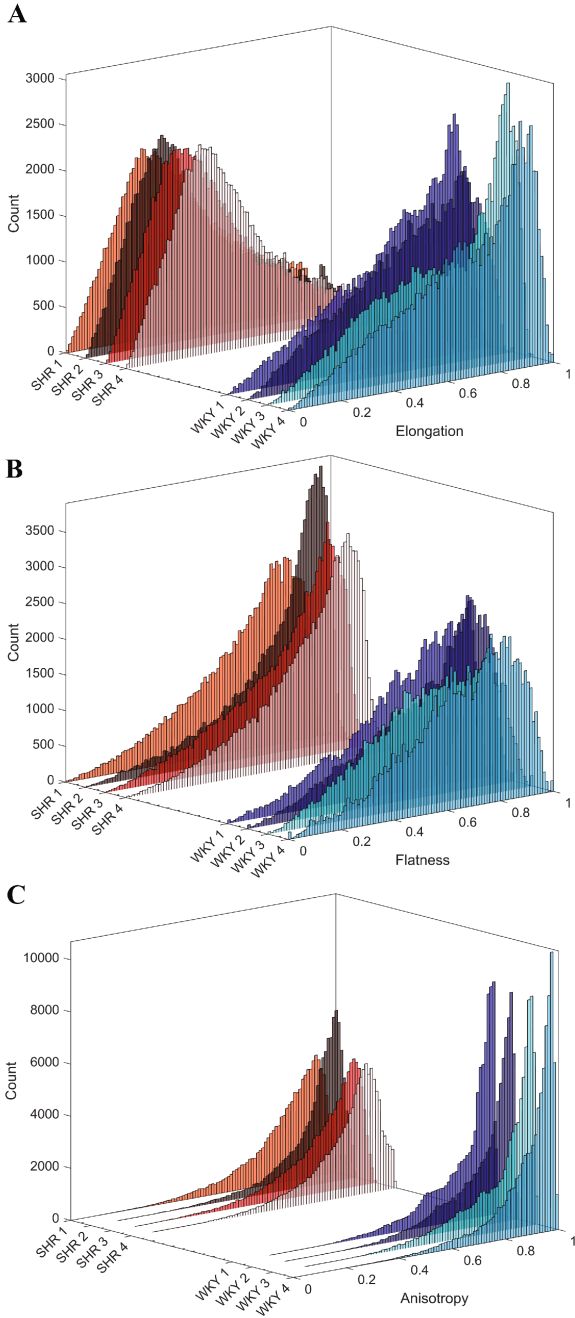


Fig. 4. 1D distributions of the (A) elongation, (B) flatness, (C) anisotropy parameters among tissue blocks from WKY (blues) and SHR (reds) hearts. (Color figure online)

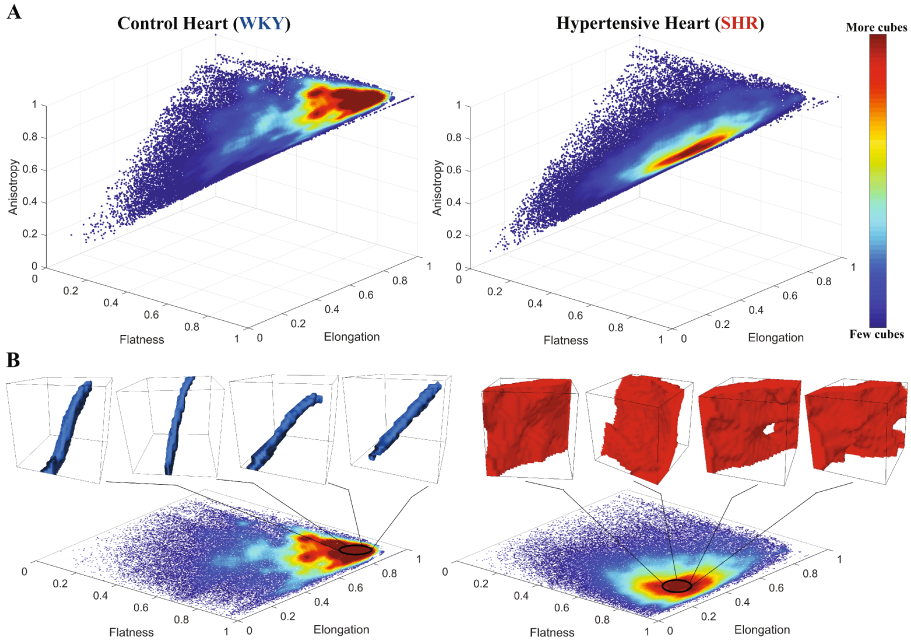


Fig. 5. Heatmap visualisation of the distributions of morphological parameters in (A) 3D and (B) in the elongation-flatness plane for heart tissue blocks from WKY (*left*) and SHR (*right*), with typical collagen shapes from the core of each heatmap

4 Conclusions

We have developed an automated method to quantify the 3D myocardial collagen morphology from confocal images using three morphological parameters. Using multiple confocal images from control and hypertensive hearts, we have shown that the proposed framework can effectively quantify the collagen shape in 3D, and can distinguish the structural remodelling of the collagen network during development and disease. In particular, our quantitative analysis revealed that the collagen structure in the diseased hearts was more sheet-like in comparison to the elongated collagen structure of the age-matched control hearts. The microstructural parameters measured in this study will be used in future computational models of the myocardium to link the observed changes in cardiac microstructure to changes in ventricular function. Such models could help to improve our understanding of the pathophysiological processes underpinning heart diseases and pave the way towards more effective treatments that target the underlying mechanisms.

References

1. Weber, K.T., Sun, Y., Tyagi, S.C., Cleutjens, J.P.: Collagen network of the myocardium: function, structural remodeling and regulatory mechanisms. *J. Mol. Cell. Cardiol.* **26**, 279–292 (1994)
2. Berk, B.C., Fujiwara, K., Lehoux, S.: ECM remodeling in hypertensive heart disease. *J. Clin. Invest.* **117**, 568–575 (2007)
3. Omens, J.H., Miller, T.R., Covell, J.W.: Relationship between passive tissue strain and collagen uncoiling during healing of infarcted myocardium. *Cardiovasc. Res.* **33**, 351–358 (1997)
4. Kato, S., Spinale, F.G., Tanaka, R., Johnson, W., Cooper, G., Zile, M.R.: Inhibition of collagen cross-linking: effects on fibrillar collagen and ventricular diastolic function. *Am. J. Physiol. Heart Circulatory Physiol.* **269**, H863–H868 (1995)
5. Brilla, C.G., Janicki, J., Weber, K.: Cardioreparative effects of lisinopril in rats with genetic hypertension and left ventricular hypertrophy. *Circulation* **83**, 1771–1779 (1991)
6. LeGrice, I.J., Pope, A.J., Sands, G.B., Whalley, G., Doughty, R.N., Smaill, B.H.: Progression of myocardial remodeling and mechanical dysfunction in the spontaneously hypertensive rat. *Am. J. Physiol. Heart Circulatory Physiol.* **303**, H1353–H1365 (2012)
7. Sands, G.B., Gerneke, D.A., Hooks, D.A., Green, C.R., Smaill, B.H., LeGrice, I.J.: Automated imaging of extended tissue volumes using confocal microscopy. *Microsc. Res. Tech.* **67**, 227–239 (2005)
8. Young, A., LeGrice, I., Young, M., Smaill, B.: Extended confocal microscopy of myocardial laminae and collagen network. *J. Microsc.* **192**, 139–150 (1998)
9. Weickert, J., Romeny, B.T.H., Viergever, M.A.: Efficient and reliable schemes for nonlinear diffusion filtering. *IEEE Trans. Image Process.* **7**, 398–410 (1998)
10. Kapur, J.N., Sahoo, P.K., Wong, A.K.: A new method for gray-level picture thresholding using the entropy of the histogram. *Comput. Vision Graph. Image Process.* **29**, 273–285 (1985)
11. Rangayyan, R.M.: *Biomedical Image Analysis*. CRC Press, Boca Raton (2004)
12. Loncaric, S.: A survey of shape analysis techniques. *Pattern Recogn.* **31**, 983–1001 (1998)
13. Flusser, J., Zitova, B., Suk, T.: *Moments and Moment Invariants in Pattern Recognition*. Wiley, Hoboken (2009)
14. El Moumen, A., Kanit, T., Imad, A., El Minor, H.: Effect of reinforcement shape on physical properties and representative volume element of particles-reinforced composites: Statistical and numerical approaches. *Mech. Mater.* **83**, 1–16 (2015)
15. Pope, A.J., Sands, G.B., Smaill, B.H., LeGrice, I.J.: Three-dimensional transmural organization of perimysial collagen in the heart. *Am. J. Physiol. Heart Circulatory Physiol.* **295**, H1243–H1252 (2008)